J. Electroanal. Chem., 133 (1982) 1–23
Elsevier Sequoia S.A., Lausanne—Printed in The Netherlands

THEORETICAL ANALYSIS OF ELECTROCHEMICAL REACTIONS INVOLVING TWO SUCCESSIVE ONE-ELECTRON TRANSFERS WITH DIMERIZATION OF INTERMEDIATE–APPLICATION TO NAD^+/NADH REDOX COUPLE

ZDENEK SAMEC *, WILLIAM T. BRESNAHAN ** and PHILIP J. ELVING

Department of Chemistry, University of Michigan, Ann Arbor, MI 48109 (U.S.A.)

(Received 21st April 1981; in revised form 7th September 1981)

ABSTRACT

The mechanism of an electrode reaction consisting of two successive one-electron (1*e*) transfer steps, coupled with dimerization of the intermediate product under conditions of steady-state convective diffusion, has been theoretically analyzed for the situation where the second electron-transfer step is accompanied or preceded by protonation of the intermediate product. The resulting relationships have been used to examine the electrochemical behavior of the biologically important NAD^+/NADH redox couple. The model, which seems best to fit the experimental data involves: (a) 1*e* reduction of NAD^+ to NAD, which can dimerize, followed at more negative potential by concerted protonation and 1*e* reduction of NAD to NADH, where the proton donor is an HB species such as H_3O^+ or NH_4^+; (b) an apparently single-step 2*e* oxidation of NADH to NAD^+. Possible causes for the differences in electrochemical NAD^+ reduction and NADH oxidation are considered in terms of the implications of theory.

INTRODUCTION

There has been increasing interest in examining the electrochemical reduction of nicotinamide adenine dinucleotide (NAD^+; DPN^+; coenzyme I), and the electrochemical oxidation of 1,4-dihydronicotinamide adenine dinucleotide (NADH; DPNH; coenzyme I reduced) from the analytical viewpoint, and as a possible basis for more thoroughly elucidating the role of the NAD^+/NADH redox couple in biological redox processes (cf. refs. cited in ref. 1). However, there is still uncertainty concerning the exact nature of the mechanisms involved, e.g. possible causes for the cathodic reduction of NAD^+ involving two one-electron (1*e*) steps well separated in potential and the anodic oxidation of NADH involving a single 2*e* step at a considerably more positive potential, whereas the grossly reversible enzymatic 2*e*

* Permanent address: J. Heyrovský Institute of Physical Chemistry and Electrochemistry, U továrven 254, 10200 Prague 10, Hostivář, Czechoslovakia.
** Present address: Research Center, Hercules Inc., Wilmington, DE 19899, U.S.A.

0022-0728/82/0000–0000/$02.75

oxidation and reduction occur at pH 7 at a computed formal potential roughly intermediate between the electrochemical reduction and oxidation potentials.

The present paper is an attempt to modify existing theory for electrode reaction mechanisms so as to make it applicable for the most general situations which may be involved in the $NAD^+/NADH$ redox system, and then to examine this system on the basis of the theory, evaluating, in so far as it may now be possible, the energetic and kinetic parameters for the individual steps in the overall redox processes, and indicating the type of additional information needed, thereby furnishing objectives for future research.

FORMULATION OF MECHANISTIC MODEL FOR NADH/NAD^+ COUPLE

The reduction of NAD^+ at mercury electrodes and the oxidation of NADH at solid electrodes* proceed according to the overall reaction,

$$NAD^+ + 2e + H^+ = NADH \quad (1)$$

The mechanism, which best accounts for the electrochemical reduction of NAD^+ [1] consists of two 1*e* steps with rapid dimerization of the intermediate radical NAḊ, i.e. schematically:

$$A + e \rightleftarrows B \quad (2)$$

$$B + e + HX \rightleftarrows C + X^- \quad (3)$$

$$2\,B \rightarrow B_2 \quad (4)$$

where A represents NAD^+, B the NAḊ radical, HX a general proton donor, C NADH and B_2 the dimer $(NAD)_2$.

At present, it is not clear whether proton and electron transfer to the NAḊ radical occur in one step (eqn. 3) or whether NAḊ is protonated before electron uptake. The most recent investigation of NADH oxidation at GC and Pt electrodes [2] indicates that the primary product is protonated $NA\dot{D}H^+$, which deprotonates relatively slowly to NAḊ. Thus, in addition to the single step described by eqn. (3), the following sequence will also be considered:

$$B + HX \rightleftarrows BH^+ + X^- \quad (5)$$

$$BH^+ + e \rightleftarrows C \quad (6)$$

The presence in the mechanism of a second bimolecular reaction, i.e. eqn. (3) or (5), greatly complicates the theoretical analysis. Therefore, we shall assume that, to a first approximation, two conditions are fulfilled:

(1) The solution is so well buffered that the concentrations of proton donor HX and proton acceptor X^-, i.e. c^0_{HX} and $c^0_{X^-}$, are constant in the whole solution including the diffusion and reaction layers.

(2) When protonation of the eqn. (5) type is involved, it is completely mobile so

---

* Abbreviations used for solid electrodes: Au, gold; GC, glassy or vitreous carbon; Pt, platinum.

that in the whole solution space the concentrations of B and BH^+, i.e. c_B and c_{BH^+}, satisfy the equilibrium:

$$K_H = c_{BH^+} c_X^0 / c_B c_{HX}^0 \tag{7}$$

where K_H is the equilibrium constant for protonation reaction (5).

In view of the rather slow deprotonation of $NADH^+$ seen for NADH oxidation at solid electrodes [2], the latter assumption may not be justified. On the other hand, the limiting current due to the second electron uptake in NAD^+ reduction at mercury electrodes does not seem to be influenced by the slow preceding chemical reaction [1].

THEORY FOR THE MECHANISTIC MODEL

Jacq [3] has considered the mechanism consisting of two successive 1*e* transfer steps coupled with dimerization of the intermediate. Assuming that (1) the equilibrium in reaction (4) is shifted towards the dimer and (2) the dimerization is sufficiently rapid that the reaction layer thickness μ is small compared with that of the Nernst diffusion layer δ, the current–potential relationship was derived by applying the approximate method of Brdička et al. [4]. The resulting equation * can be easily modified for the mechanistic model just outlined. Thus, if the dimerization of eqn. (4) is completely irreversible, the equation for the current–potential curve is

$$Y^3 = 3X^2/4\lambda^2 \tag{8}$$

where X and Y are functions, expressed by eqns. (9) and (10), of the dimensionless current J and of the dimensionless kinetic parameters λ, a and b:

$$X = \left\{(a+b)J - 2\left(p/p' - q'c_C^0/qc_A^0\right)\right\}/(a-b) \tag{9}$$

$$Y = \left\{abJ - bp/p' + aq'c_C^0/qc_A^0\right\}/(a-b) \tag{10}$$

The dimensionless current J is defined by

$$J = -I/\left(FAD\,\delta^{-1}c_A^0\right) \tag{11}$$

where I is the current, F the Faraday constant, A the electrode area, D the diffusion coefficient and C_A^0 the bulk concentration of NAD^+. The thickness of the diffusion layer at the rotating disc electrode (RDE), δ(RDE), is given [5] by

$$\delta(\mathrm{RDE}) = 1.61 D^{1/3} \nu^{1/6} \omega^{-1/2} \tag{12}$$

where ν is the kinematic viscosity and ω the angular rotation velocity. For the dropping mercury electrode, the classical expression involving the drop-time t can be used:

$$\delta(\mathrm{DME}) = (3\pi Dt/7)^{1/2} \tag{13}$$

* Equation (20) in ref. 3 for the current–potential curve involves a significant typographical error: Y^3/S should be read as $Y^2/3$.

If the mechanism of eqns. (2)–(4) is considered, the kinetic parameter λ is given by

$$\lambda^2 = \delta^2 k_d c_A^0 D^{-1} \tag{14}$$

where k_d is the dimerization rate constant, while for the mechanism of eqns. (2) and (4)–(6),

$$\lambda^2 = \left(1 + K_H c_{HX}^0 / c_{X^-}^0\right) \delta^2 k_d c_A^0 D^{-1} \tag{15}$$

The kinetic parameters a and b are defined by

$$a = (1+p)/p' \tag{16}$$

$$b = (1+q')/q \tag{17}$$

where p, p', q and q' are the dimensionless rate constants for the electron-transfer steps, i.e.

$$\begin{aligned} p &= k_1 \delta D^{-1} \\ p' &= k_1' \delta D^{-1} \\ q &= k_2 \delta D^{-1} \\ q' &= k_2' \delta D^{-1} \end{aligned} \tag{18}$$

The cathodic, k_n, and anodic, k_n', rate constants depend on the electrode potential E. For the first electron uptake described by eqn. (2), these dependences are given by

$$k_1 = k_1^0 \exp\left[-\alpha_1 F\left(E - E_1^0\right)/RT\right] \tag{19}$$

$$k_1' = k_1^0 \exp\left[(1-\alpha_1) F\left(E - E_1^0\right)/RT\right] \tag{20}$$

where k_1^0 is the apparent rate constant, E_1^0 the formal redox potential of reaction (2) and α_1 the apparent cathodic charge-transfer coefficient.

If the second electron uptake proceeds according to eqn. (3), the cathodic, k_2, and anodic, k_2', rate constants are given by

$$k_2 = k_2^0 c_{HX}^0 \exp\left[-\alpha_2 F\left(E - E_2^0\right)/RT\right] \tag{21}$$

$$k_2' = k_2^0 c_{X^-}^0 \exp\left[(1-\alpha_2) F\left(E - E_2^0\right)/RT\right] \tag{22}$$

where the parameters k_2^0, α_2 and E_2^0 refer to reaction (3) and have the similar significance as above, but k_2^0 is now a second-order rate constant.

If, alternatively, the second electron transfer proceeds according to eqn. (6), the potential-dependent rate constants are

$$k_2 = k_2^0 \left(k_H c_{HX}^0 / c_{X^-}^0\right) \exp\left[-\alpha_2 F\left(E - E_2^0\right)/RT\right] \tag{23}$$

$$k_2' = k_2^0 \exp\left[(1-\alpha_2) F\left(E - E_2^0\right)/RT\right] \tag{24}$$

Consequences following from the general equation for the current–potential curve were only briefly mentioned by Jacq [3]. The simplified scheme involving a single electron-transfer step with dimerization of the product was considered by Bonna-

terre and Cauquis [6], who derived and discussed the equation for the current–potential curve, using a method similar to that in refs. 3 and 7. Therefore, it is in order to analyze eqn. (8) in detail. The relevant experiments are usually performed under such conditions that only one component has a non-zero bulk concentration. Consequently, the cathodic and anodic reactions can be considered separately. It is useful to realize that the functions X and Y have a straightforward meaning inasmuch as they are directly related to the dimensionless concentrations of B and B_2 at the electrode surface, i.e. c_B^* and $c_{B_2}^*$ [3,7]:

$$Y = c_B^*/c_A^0 \geqslant 0 \tag{25}$$

$$X \simeq -2c_{B_2}^*/c_A^0 \leqslant 0 \tag{26}$$

Cathodic electrode reaction

The bulk concentrations of all components except that of A are assumed to be zero. The steady-state current–potential curve is given by eqn. (8), with X and Y being given by

$$X = \frac{(a+b)J - 2p/p'}{a-b} \leqslant 0 \tag{27}$$

$$Y = \frac{abJ - bp/p'}{a-b} \geqslant 0 \tag{28}$$

Analysis of the current–potential relationship can be based on the differing dependencies of kinetic parameters a and b on the electrode potential E; a exponentially decreases and b exponentially increases with increasingly positive E (cf. eqns. 16–22). The two functions, $a(E)$ and $b(E)$, intersept at $E = E^*$.

(1) Case for $E > E^*$

If $E > E^*$ so that $b \gg a$,

$$X = -J + 2p/p'b \leqslant 0 \tag{29}$$

$$Y = -aJ + p/p' \geqslant 0 \tag{30}$$

The inequalities (29) and (30), together with $b \gg a$, indicate that the dimensionless current J satisfies the inequality:

$$p/(1+p) \geqslant J \geqslant 2p/p'b \simeq 0 \tag{31}$$

It should be noted that $J = p/(1+p)$ is the equation for the irreversible cathodic wave corresponding to reaction (2) alone, i.e. without coupled chemical or electrochemical reactions (3) or (4).

By inserting eqns. (29) and (30) into eqn. (8) and neglecting the term $2p/p'b$, the current–potential equation is obtained in the form:

$$J = \frac{p}{1+p} - \frac{p'}{1+p}\left(\frac{3}{4\lambda^2}\right)^{1/3} J^{2/3} \tag{32}$$

If E can be made sufficiently negative so that $p \gg 1$ but the inequality $b \gg a$ still holds, J approaches $J_l = 1$ and the limiting current I_l is given by (cf. eqn. 11)

$$I_l = -FAD\,\delta^{-1}c_A^0 \tag{33}$$

In this case, eqn. (32) is the equation for the 1*e* cathodic wave corresponding to reaction (2) followed by dimerization of its product (eqn. 4). Equation (32) can be rewritten as

$$\frac{I_l - I}{I} = \frac{D}{\delta k_l^0}\exp\left[\alpha_l F\left(E - E_l^0\right)/RT\right] + \left(\frac{4\lambda^2 I}{3I_l}\right)^{-1/3}\exp\left[F\left(E - E_l^0\right)/RT\right] \tag{34}$$

which coincides with the equation derived for this case by Bonnaterre and Cauquis [6].

As discussed in ref. 6, the plot of $\log[(I_l - I)I^{-}]$ vs. E (the logarithmic or log analysis) has generally two limiting reciprocal slopes: $(2/3)(2.303RT/F)$ for $E \to \infty$ and $2.303RT/\alpha_l F$ for $E \to -\infty$. When the first term on the right-hand side of eqn. (34) considerably exceeds the second term in the potential region where log analysis of the cathodic wave can be performed with sufficient accuracy (usually for I/I_l between 0.1 and 0.9), only the latter limiting slope is found and the half-wave potential $E_{l/2}^{irr}$ is given by

$$E_{l/2}^{irr} = E_l^0 + (2.303RT/\alpha_l F)\log\left(k_l^0\,\delta D^{-1}\right) \tag{35}$$

which is the expression for $E_{l/2}$ of the cathodic wave corresponding only to irreversible electron-transfer reaction (2).

If, on the other hand, the second term on the right-hand side of eqn. (34) prevails, eqn. (34) is better rewritten as

$$I^{2/3}I_l^{1/3}/(I_l - I) = \tfrac{4}{3}\lambda^2\exp\left[-F\left(E - E_l^0\right)/RT\right] \tag{36}$$

The plot of $\log[I^{2/3}I_l^{1/3}/(I_l - I)]$ vs. E is linear with the reciprocal slope of $2.303RT/F$* and

$$E_{l/2}^{rev} = E_l^0 + (2.303RT/3F)\log\left(\tfrac{2}{3}\lambda^2\right) \tag{37}$$

The dependence of $E_{l/2}^{rev}$ on the bulk concentration of A through λ^2 (cf. eqn. 14 or 15) is characterized by the slope:

$$\Delta E_{l/2}^{rev}/\Delta \log c_A^0 = 2.303RT/3F \tag{38}$$

When protonation reaction (5) occurs, $E_{l/2}^{rev}$ will also depend on the concentrations of

---

* In comparing eqn. (36) with the similar equation on p. 206 of ref. 6, namely,

$$E = E^0 - (RT/F)\ln\left[j^{2/3}(j_d - j)^{-1}\right] - (RT/3F)\ln\left[\tfrac{2}{3}FD\,\delta^{-1}\lambda_F^{-2}\left(c_A^0\right)^{-1}\right]$$

where j is the current density; the different definition of $\lambda_F^2 = (2\lambda^2/c_A^0)$ (cf. eqn. 2 of ref. 6) and the incorrect presence of concentration c_A^0 in the last term on the right-hand side of the latter equation should be noted.

proton donor HX and proton acceptor, X^-:

$$\Delta E_{1/2}^{rev}/\Delta \log c_{HX}^0 = (2.303RT/3F)\frac{K_H c_{HX}^0/c_{X^-}^0}{1+K_H c_{HX}^0/c_{X^-}^0} \quad (39)$$

$$\Delta E_{1/2}^{rev}/\Delta \log c_{X^-}^0 = -(2.303RT/3F)\frac{K_H c_{HX}^0/c_{X^-}^0}{1+K_H c_{HX}^0/c_{X^-}^0} \quad (40)$$

Once the value of $E_{1/2}^{rev}$ is determined and that of E_1^0 is known, dimerization rate constant k_d can be evaluated from eqn. (37).

If, in the potential region $E > E^*$, E cannot be made sufficiently negative to fulfil the inequality $p \gg 1$, J is given by the more general eqn. (32) and does not reach the limiting value.

(2) Case for $E < E^*$

In the potential region $E < E^*$, where $b \ll a$, eqns. (27) and (28) simplify so that X and Y are given by

$$X = J - 2p/(1+p) \leqslant 0 \quad (41)$$

$$Y = b\left(J - \frac{p}{1+p}\right) \geqslant 0 \quad (42)$$

and J apparently satisfies the inequalities:

$$p/(1+p) \leqslant J \leqslant 2p/(1+p) \quad (43)$$

No restrictions are now imposed on E towards its negative limit, i.e. $E \to \infty$, and, therefore, $j_l = 2$ can be achieved and

$$I_l = -2FAD\delta^{-1}c_A^0 \quad (44)$$

By use of eqns. (41), (42) and (8) we obtain:

$$\left(J - \frac{p}{1+p}\right)/\left(\frac{2p}{1+p} - J\right)^{2/3} = \left(\frac{3}{4\lambda^2}\right)^{1/3} b^{-1} \quad (45)$$

which, as compared with eqn. (32), also involves the parameter b for the second electron-transfer reaction and is accordingly more complex.

We can again consider the situation that, in the potential region $E > E^*$, E can be made sufficiently negative for parameter p to satisfy the inequality $p \gg 1$. This inequality must naturally also hold in the potential region $E < E^*$ and eqn. (45) simplifies to

$$\frac{(J-1)}{(2-J)^{2/3}} = \left(\frac{3}{4\lambda^2}\right)^{1/3} b^{-1} \quad (46)$$

It is appropriate at this point to introduce the dimensionless current J' defined by

$$J' = J - 1 \quad (47)$$

which approaches unity for $E \to -\infty$; the limiting current I_l' is given by eqn. (33).

Substitution of eqn. (47) into eqn. (46) gives

$$J'/(1-J')^{2/3} = (3/4\lambda^2)^{1/3} b^{-1} \tag{48}$$

which is the equation for the 1*e* cathodic wave corresponding to second electron-transfer reaction (3) or (6) preceded by dimerization reaction (4) and, eventually, by protonation reaction (5).

In order to analyze eqn. (48), the mechanism for proton involvement must be specified. Thus, if simultaneous proton and electron addition to B occurs (eqn. 3), eqn. (48) has the form:

$$\frac{I(I_l')^{-1/3}}{(I_l'-I)^{2/3}} = \left(\frac{3}{4\lambda^2}\right)^{1/3} \frac{k_2^0\,\delta D^{-1} c_{HX}^0 \exp\left[-\alpha_2 F(E-E_2^0)/RT\right]}{1+k_2^0\,\delta D^{-1} c_{X^-}^0 \exp\left[(1-\alpha_2)F(E-E_2^0)/RT\right]} \tag{49}$$

The plot of $\log[I(I_l')^{-1/3}/(I_l'-I)^{2/3}]$ vs. E has, in general, two reciprocal slopes: $-2.303RT/F$ for $E \to \infty$ and $-2.303RT/\alpha_2 F$ for $E \to -\infty$. The former slope can obviously be found in the region $E < E^*$ only when E_2^0 is sufficiently negative to E_1^0. In the reverse case, i.e. $E_2^0 > E_1^0$, only the cathodic wave corresponding to the irreversible second electron-transfer step can be found in the region $E < E^*$ ($b \ll a$). The equation is then:

$$\frac{I(I_l')^{-1/3}}{(I_l'-I)^{2/3}} = \left(\frac{3}{4\lambda^2}\right)^{1/3} \left(k_2^0\,\delta D^{-1} c_{HX}^0\right) \exp\left[-\alpha_2 F(E-E_2^0)/RT\right] \tag{50}$$

$E_{1/2}$ for this irreversible wave is given by

$$E_{1/2}^{irr} = E_2^0 + \frac{2.303RT}{\alpha_2 F} \log\left(k_2^0\,\delta D^{-1} c_{HX}^0\right) + \frac{2.303RT}{3\alpha_2 F} \log\left[\left(\tfrac{3}{2}\right)\lambda^{-2}\right] \tag{51}$$

and obviously depends on the bulk concentrations of both A and HX. These dependencies are characterized by the slopes:

$$\Delta E_{1/2}^{irr}/\Delta \log c_A^0 = -(2.303RT/3\alpha_2 F) \tag{52}$$

$$\Delta E_{1/2}^{irr}/\Delta \log c_{HX}^0 = 2.303RT/\alpha_2 F \tag{53}$$

Similar equations can be written for the mechanisms involving protonation of B (eqn. 5), followed by electron-transfer reaction (6).

In place of eqn. (49) we have:

$$\frac{I(I_l')^{-1/3}}{(I_l-I)^{2/3}} = \left(\frac{3}{4\lambda^2}\right)^{1/3} \frac{k_2^0\,\delta D^{-1}\left(K_H c_{HX}^0/c_{X^-}^0\right) \exp\left[-\alpha_2 F(E-E_2^0)/RT\right]}{1+k_2^0\,\delta D^{-1} \exp\left[(1-\alpha_2)F(E-E^0)/RT\right]} \tag{54}$$

where λ is given by eqn. (15) and, analogously, instead of eqns. (50) and (51), we have:

$$\frac{I(I_l')^{-1.3}}{(I_l'-I)^{2/3}} = \left(\frac{3}{4\lambda^2}\right)^{1/3} \left(k_2^0\,\delta D^{-1} K_H c_{HX}^0/c_{X^-}^0\right) \exp\left[-\alpha_2 F(E-E_2^0)/RT\right] \tag{55}$$

$$E_{1/2}^{irr} = E_2^0 + \frac{2.303RT}{\alpha_2 F} \log\left(k_2^0 \delta D^{-1} K_H c_{HX}^0 / c_{X^-}^0\right) + \frac{2.303RT}{3\alpha_2 F} \log\left[\left(\tfrac{3}{2}\right)\lambda^{-2}\right] \quad (56)$$

The dependence of $E_{1/2}^{irr}$ on the concentration of A is given by eqn. (52) and on the concentrations of HX and X^- by

$$\frac{\Delta E_{1/2}^{irr}}{\Delta \log c_{HX}^0} = \frac{2.303RT}{\alpha_2 F} - \frac{2.303RT}{3\alpha_2 F} \frac{\left(K_X c_{HX}^0 / c_{X^-}^0\right)}{\left(1 + K_H c_{HX}^0 / c_{X^-}^0\right)} \quad (57)$$

$$\frac{\Delta E_{1/2}^{irr}}{\Delta \log c_{X^-}^0} = -\frac{2.303RT}{\alpha_2 F} + \frac{2.303RT}{3\alpha_2 F} \frac{\left(K_H c_{HX}^0 / c_{X^-}^0\right)}{\left(1 + K_H c_{HX}^0 / c_{X^-}^0\right)} \quad (58)$$

On the other hand, when the parameter p does not satisfy the inequality $p \gg 1$ in the potential region $E > E^*$, J in this potential region is given by the more general eqn. (45).

Anodic electrode reaction

The bulk concentrations of all components except C are to be assumed to be zero. The dimensionless concentrations of intermediates X and Y (eqns. 25 and 26) are now related to c_C^0 and, analogously, J and λ are given by eqns. (59) and (60) instead of eqns. (11) and (14):

$$J = I/\left(FAD\,\delta^{-1} c_C^0\right) \quad (59)$$

$$\lambda^2 = \delta^2 k_d c_C^0 D^{-1} \quad (60)$$

When these changes are made in eqns. (9) and (10) by multiplying both sides of the equations by (c_A^0/c_C^0), we can proceed in the same way as for the cathodic electrode reaction. The steady-state current–potential curve is given by eqn. (8), where X and Y result from the substitution of q' for p and of q for p' in eqns. (27) and (28), i.e. a for b and b for a:

$$X = \frac{(2q'/q) - (a+b)J}{a-b} \leqslant 0 \quad (61)$$

$$Y = \frac{(aq'/a) - abJ}{a-b} \geqslant 0 \quad (62)$$

Similar substitution in the equations for the cathodic electrode reaction current yields the equations valid for the anodic electrode reaction; consequently, only two general equations for J are given:

(1) If $E < E^*$ so that $a \gg b$, J satisfies the inequalities:

$$\frac{q'}{1+q'} \geqslant J \geqslant \frac{2q'}{aq} \simeq 0 \quad (63)$$

and is given, analogously to eqn. (32), by

$$J = \frac{q'}{1+q'} - \frac{q}{1+q'}\left(\frac{3}{4\lambda^2}\right)^{2/3} J^{2/3} \quad (64)$$

(2) If $E > E^*$ so that $b \gg a$, J satisfies the inequalities:

$$\frac{q'}{1+q'} \leqslant J \leqslant \frac{2q'}{1+q'} \tag{65}$$

and is given, analogously to eqn. (45), by

$$\frac{J - \frac{q'}{1+q'}}{\left(\frac{2q'}{1+q'} - J\right)^{2/3}} = \left(\frac{3}{4\lambda^2}\right)^{1/3} a^{-1} \tag{66}$$

DISCUSSION OF MECHANISTIC MODEL

The question will now be considered as to the extend to which the mechanism of two successive 1*e* transfer reactions with dimerization of the intermediate product may account for the observed electrochemical behavior of the $NAD^+/NADH$ couple at both mercury and solid electrodes. The available data do not allow definitive conclusions to be drawn about either the nature of the proton donor/acceptor couple HX/X^- in the overall reaction:

$$NAD^+ + HX + 2e = NADH + X^- \tag{67}$$

or the way in which this couple is involved in the reduction of NAD· to NADH or the oxidation of NADH to NAD·. It is clear, however, that the rate of NAD· reduction at a Hg electrode increases with concentration of a proton donor such as H_3O^+ or NH_4^+. This fact is anticipated by the mechanism represented by either eqn. (3) or eqns. (5) and (6); the distinction is between successive and simultaneous proton and electron transfers to NAD·*. From a molecular viewpoint, the Franck–Condon principle applies, i.e. the electron transition occurs at a fixed configuration of the heavy particles including the proton. For the radiationless electron transition to occur, the activated complex formed must correspond to the molecular situation in which the electron energies in the initial and final states are equal within the uncertainty limit. The situation in reduction of NAD· to NADH is similar to that encountered in inner-sphere electron-transfer reactions in solution, i.e. both electron and atom transfer resulting in a significant change in molecular structure of the reacting particle are involved. Following general theoretical considerations for such electron-transfer reactions [8], formation of an activated complex such as

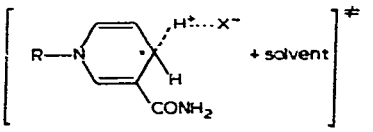

(68)

* The word "simultaneous" is used only figuratively in order to express that the proton and the electron are transferred in a single, distinct (electro)chemical step.

can be envisaged irrespective of whether a stable protonated radical $NAD^{\cdot}H^+$ is formed or the electron is immediately transferred from an energy level in the electrode to an energy level in the nicotinamide moiety to form NADH. In the former case, the activated complex corresponds to the molecular situation favorable for the radiationless rearrangement of the electronic subsystem in the $NAD^{\cdot}H^+X^-$ complex involving bond-breaking in HX and C(4)–H bond-forming in the nicotinamide moiety; $NAD^{\cdot}H^+$ and the solvent around it must subsequently undergo the proper reorganization to form an activated complex which allows the radiationless electron transfer from an electrode energy level to one in the nicotinamide moiety in $NAD^{\cdot}H^+$.

Alternatively, the activated complex (eqn. 68) corresponds to the state of the system favorable for the radiationless rearrangement of the electronic subsystem involving electron transfer from electrode to nicotinamide moiety; in this case, the stable intermediate $NAD^{\cdot}H^+$ is not formed on reduction of $NAD^{\cdot}$ to NADH, which then proceeds as a bimolecular reaction (eqn. 3).

Data on reduction of NAD^+ at Hg will be analyzed, assuming the proton donor to be H_3O^+. Estimation of all the parameters of the mechanistic model is possible only for reduction of $NAD^{\cdot}$ to NADH in a single step (eqn. 3). Analysis of the mechanism involving protonation step (5) requires knowledge of the equilibrium constant K_H for protonation of $NAD^{\cdot}$, which is not available. Possible values of the mechanistic parameters for reduction of $NAD^{\cdot}$ to NADH involving such a protonation step will be considered.

The data analysis is complicated by possible adsorption at Hg of NAD^+ and its reduction products. This problem is largely eliminated when excess tetraethylammonium cation (Tea^+) is present. Therefore, only polarographic and voltammetric data obtained at Hg in 0.4 *M* TeaCl, carbonate buffer (pH 9–10) [9,10; present study via ref. 11] will be considered.

Formal potential for NAD^+/NADH

The formal potential, E^0, of the NAD^+/NADH couple is related to the formal potentials of the NAD^+/$NAD^{\cdot}$ and $NAD^{\cdot}$/NADH redox couples, E_1^0 and E_2^0, respectively,

$$E^0 = \left(E_1^0 + E_2^0\right)/2 \tag{69}$$

The formal potential, $E_2^{0\prime}$, of the $NAD^{\cdot}H^+$/NADH couple can be calculated from E_2^0 and the protonation equilibrium constant, K_H:

$$E_2^0 = E_2^{0\prime} + (RT/F)\ln K_H \tag{70}$$

At pH 7 and 25°C, the apparent formal potential $E^{0\prime}$ of the NAD^+/NADH couple:

$$E^{0\prime} = E^0 + (RT/2F)\ln\left(c^0_{H_3O^+}/c^0_{H_2O}\right) \tag{71}$$

is −0.315 V vs. NHE [12] or −0.557 V vs. SCE. On insertion of $c^0_{H_3O^+} = 10^{-7}\,M$ and $c^0_{H_2O} = 55.5\,M$ in eqn. (71), $E^0 = -0.295$ V (SCE).

Diffusion coefficients

The NAD^+ diffusion coefficient, D, can be calculated from the maximum limiting current, I_l, of the wave due to 1e reduction of NAD^+ to NAD̈:

$$D = \left[I_l / 708.1 m^{2/3} t_l^{1/6} c^0 \right]^2 \tag{72}$$

where I_l is in μA, c^0 is the bulk NAD^+ concentration in mM, m the Hg flow-rate in mg s^{-1} and t_l the Hg drop-time in s. The mean value of D, 3.5×10^{-6} cm^2 s^{-1}, calculated from four measurements at 0.204–1.48 mM NAD^+, agrees well with those of 4.3×10^{-6} and 3.4×10^{-6} cm^2 s^{-1} previously reported for aqueous media (ref. 1, p. 8). From measurement of I_l for NADH oxidation at GC, Pt and Au RDEs, D for NADH was calculated to be 3.3×10^{-6} cm^2 s^{-1} [13].

Parameters for mechanistic model for $NAD^+/NA\dot{D}$ couple

The reduction of NAD^+ to NAD̈ with subsequent dimerization of NAD̈ is well separated in potential at an Hg electrode from the reduction of NAD̈ to NADH; accordingly, its analysis may proceed independently of the analysis of the latter process, except for the effect of pH. As previously discussed, when protonation reaction (5) occurs, $E_{1/2}$ for cathodic wave I corresponding to the reversible $NAD^+/NA\dot{D}$ reaction should depend on concentration of the proton donor H_3O^+ (eqn. 39). Experimentally, however, only negligible pH dependence is found [9], which would correspond either to $k_H c^0_{H_3O^+}/c^0_{H_2O} \ll 1$ or to simultaneous proton and electron transfer on reduction of NAD̈ to NADH (eqn. 3).

The parameters of the mechanistic model for the $NAD^+/NA\dot{D}$ couple (i.e. formal potential E_l^0, apparent rate constant k_l^0, apparent charge-transfer coefficient α_l and dimerization rate constant k_d), can be evaluated from data obtained by cyclic voltammetry at a hanging mercury drop electrode (HMDE) and polarography at a dropping mercury electrode (DME).

(1) Cyclic voltammetry

The theoretically expected behavior on cyclic voltammetry of a reversible electron-transfer reaction followed by irreversible dimerization of the product [14] is characterized by the variation of the cathodic peak current function J_{pc} (eqn. 73), the cathodic peak potential E_{pc} and the anodic–cathodic peak current ratio I_{pa}/I_{pc} with the variable parameter ψ (eqn. 74), where v is the polarization rate:

$$J_{pc} = I_p / 602 A D^{1/2} v^{1/2} c^0 \tag{73}$$

$$\psi = k_d c^0 RT / Fv \tag{74}$$

J_{pc} varies only slightly with ψ, approaching limits of 0.526 at high ψ (low v) and 0.446 at low ψ (high v).

Here E_{pc} depends on both v and c^0 at the sufficiently low values of v, which satisfy the condition of $\psi \gtrsim 10$:

$$E_{pc} = E_l^0 + (RT/3F)[\ln \psi - 3.12] \tag{75}$$

At sufficiently high v (low ψ), $E_{pc} - E_l^0$ approaches the value found for the reversible electron-transfer reaction alone, i.e.

$$E_{pc} = E_l^0 - 0.0285 \tag{76}$$

The peak current ratio is a function of the quantity, $\log(\psi nFv\tau/RT) = \log(k_d c^0 \tau)$, where τ is the time from E_l^0 to the cyclic voltammetric switching potential E_2, and varies from zero at sufficiently low v, where dimerization outruns the oxidation reaction, to one at high v, where oxidation outruns dimerization.

The cyclic voltammetric behavior of 0.20 and 0.40 mM NAD^+ in 0.4 M TeaCl and 62.5 mM carbonate buffer (starting potential -0.9 V) was examined for $v = 0.075$–616 V s^{-1}.

The experimental cathodic peak current function, $I_{pc}/Acv^{1/2}$, varies only slightly with v; the mean value is 450 μA $s^{1/2}$ cm^{-2} mM^{-1} $V^{-1/2}$ at low v and 425 at high v. The corresponding calculated D values for NAD^+ are 2.1×10^{-6} and 2.5×10^{-6} cm^2 s^{-1}, respectively; these are somewhat lower than those obtained from the DME I_l. However, the necessary correction for background current introduces a 5–7% error in the limiting and peak currents, resulting in a 10–15% error in D, i.e. a possible difference in D from the two methods of 20–30%.

In Fig. 1, the function $E_{pc} - 0.0197 \log c^0$ is plotted vs. $\log v$. At $v < 1$ V s^{-1}, the points for all three NAD^+ concentrations fall on the same straight line for which regression analysis yields a slope of -16 mV, from which the value of $E_l^0 + 0.0197 \log k_d = -0.996$ V can be inferred using eqn. (75). On the other hand, the function does not reach the limit expected at high v, because it is then controlled by the electron-transfer step; this is supported by anodic–cathodic peak potential separation of 65–80 mV at high v.

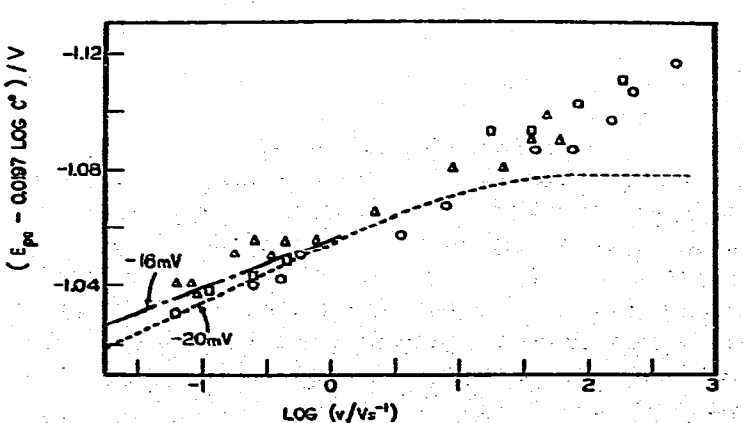

Fig. 1. Variation of the function $E_{pc} - 0.0197 \log c^0$ with polarization rate, v, for the more positive cathodic peak of NAD^+ on cyclic voltammetry at a HMDE (area = 0.0183 cm^2) at following NAD^+ concentration, c^0: (△) 0.049 mM; (○) 0.20 mM; (□) 0.40 mM. (— — —) Theoretical dependence calculated from ref. 14 for $c^0 = 0.20$ mM, $E_l^0 = -1.123$ V and $k_d = 2.7 \times 10^6$ M^{-1} s^{-1}; (·—·—·) linear regression from all experimental points at $v < 1$ V s^{-1}.

The fact that, at sufficiently high v, E_{pc} becomes independent of v and is related to E^0 by eqn. (76), enables calculation of both E_I^0 and k_d from a single cyclic voltammogram, if the electron-transfer step is reversible. (Positive feedback was used for iR compensation in all fast-scan cyclic voltammograms [15].)

Although the fast-scan cyclic voltammetry data on the $NAD^+/NAD^{\cdot}$ couple do not correspond strictly to a reversible electron-transfer step, the extent of control of the electrode reaction by the electron-transfer step is obviously small. The cathodic and anodic peak currents are rather insensitive to a small decline from reversibility; the more significant error in calculation of k_d from their ratio may be underestimation of the time τ.

The following procedure was used to evaluate k_d. From the peak potentials E_I^0 was inferred as $E_I^0 = (E_{pc} + E_{pa})/2$; the value of this operative formal potential depended slightly on v (35–500 V s^{-1}), i.e. -1.138 to -1.150 V. The mean k_d of $2.7 \times 10^6\ M^{-1}\ s^{-1}$ (8 experiments at 4 v and 2 concentrations) was obtained by the peak current ratio method [14]. The difference between E^0 and E_2 generally exceeded 0.1 V.

Use of $E_I^0 + 0.0197 \log k_d = -0.996$ V, obtained from slow-scan cyclic voltammetry, and $k_d = 2.7 \times 10^6\ M^{-1}\ s^{-1}$ gives $E_I^0 = -1.123$ V. The expected dependence of $E_{pc} - 0.0197 \log c^0$ on $\log v$ corresponding to the latter two values is shown by the dashed line in Fig. 1.

The operative value of E_I^0 used in the calculation of k_d is about 24 mV more negative than that found from slow-scan cyclic voltammetry; this would correspond to overestimation of k_d by 25% or less.

(2) DME polarography

Equation (34), which is relevant for evaluation of k_d, E_I^0, k_I^0 and α_I from cathodic wave I, can be written as

$$\frac{I_I - I}{I} = \exp\left[\alpha_I F\left(E - E_{I/2}^{irr}\right)/RT\right] + \left(\frac{I_I}{2I}\right)^{1/3} \exp\left[F\left(E - E_{I/2}^{rev}\right)/RT\right] \qquad (77)$$

Because $E_{1/2}$ for this wave does not appreciably depend on pH [9], the expression for λ has the form of eqn. (14) and $E_{I/2}^{irr}$ and $E_{I/2}^{rev}$ are given by eqns. (35) and (37).

On the basis of eqn. (77), plots of $\log[(I_I - I)I^{-1}]$ vs. E are expected to be curvilinear, with reciprocal slopes approaching 39 mV for $E \to \infty$ and $2.303RT/\alpha_I F$ for $E \to -\infty$. Because only the second term on the right-hand side of eqn. (77) depends on c^0, the variation in reciprocal slope with concentration can be observed in the region of $\log[(I_I - I)I^{-1}]$ between -1.3 and 1.3, where the log analysis can be reliably performed. Here $E_{1/2}$ is expected to depend on c^0, i.e.

$$0 \leqslant \Delta E_{1/2}/\Delta \log c^0 \leqslant 0.0197\ V \qquad (78)$$

In the plot of $\log[(I_I - I)I^{-1}]$ vs. E for NAD^+ wave I (Fig. 2), the reciprocal slopes for $E \to -\infty$ and ∞ are 120 and 40 mV respectively; the former slope corresponds to an α_I of 0.5.

From Fig. 2 $E_{I/2}^{rev}$ and $E_{I/2}^{irr}$ were evaluated as follows. Extrapolation of the linear

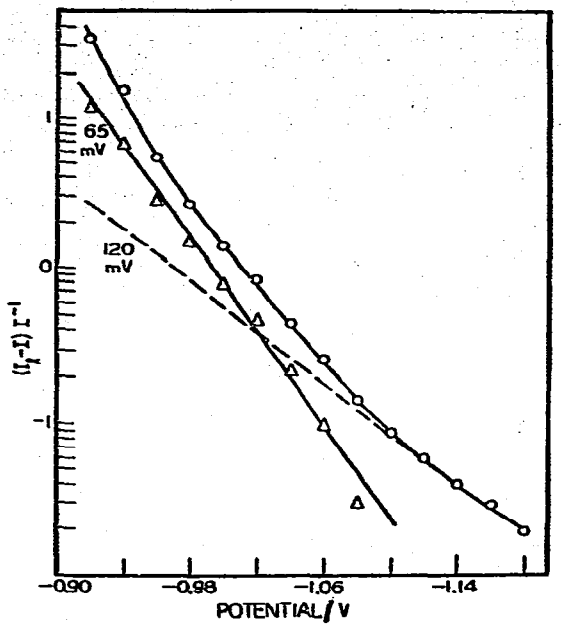

Fig. 2. (O) Plot of $\log[(I_1-I)I^{-1}]$ vs. potential E for the more positive cathodic wave of NAD^+ (0.745 mM) at a DME; (— — —) extrapolated from data at the most negative potentials. (△) plot of $\log S^{rev}$ vs. E, calculated from eqn. (79) for $\alpha_1 = 0.5$ and $E^{irr}_{1/2} = -0.97$ V.

log plot at $E \to -\infty$ to $\log[(I_1-I)I^{-1}] = 0$ gives $E^{irr}_{1/2} = -0.97$ V. Using this value and $\alpha_1 = 0.5$, a plot of $\log S^{rev}$ vs. E was constructed, where

$$S^{rev} = \left[(I_1-I)I^{-1} - \exp\left\{\alpha_1 F\left(E - E^{irr}_{1/2}\right)/RT\right\}\right](2I/I_1)^{1/3} \qquad (79)$$

Such a plot should be linear with a reciprocal slope of 59 mV; the constructed plot is linear with a reciprocal slope of 65 mV, close to that expected. At $\log S^{rev} = 0$, $E = E^{rev}_{1/2} = -0.994$ V.

The plot of $E_{1/2}$ vs. $\log c^0$ [9] is linear with a slope, $\Delta E_{1/2}/\Delta \log c^0$, of 46 mV (Fig. 3A). This value, which differs from that expected (cf. eqn. 78), indicates the limit in interpretation of the polarographic behavior in terms of the mechanism considered. In fact, $E_{1/2}$ is more positive than would correspond to the values of $k_d = 2.7 \times 10^6\ M^{-1}\ s^{-1}$ and $E^0_1 = -1.123$ V derived from cyclic voltammetry, e.g. using $E^{rev}_{1/2} = -0.994$, a value of $E^0_1 + 0.0197 \log k_d = -0.937$ V is calculated from eqn. (37), which is ca. 60 mV more positive than the −0.996 V derived from slow-scan cyclic voltammetry. This inconsistency is disturbing since the slow-scan cyclic voltammetric and the polarographic measurements involve approximately the same time-scale; it is probably due to adsorption of NAD^+ and/or its reduction products, which is not completely suppressed by adsorption of Tea^+ and which increases with increasing NAD^+ concentration and in the absence of Tea^+ (cf. polarographic behavior when K^+ replaces Tea^+ [1]).

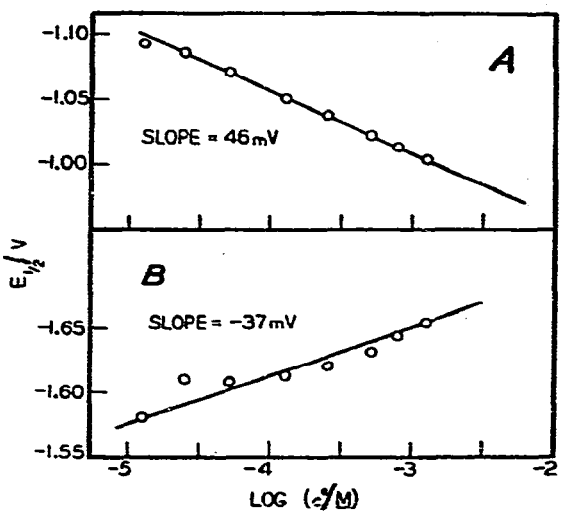

Fig. 3. Variation of $E_{1/2}$ for the more positive (A) and more negative (B) cathodic waves of NAD^+ at the DME with NAD^+ concentration c^0.

At sufficiently low NAD^+ concentration, the polarographic and cyclic voltammetric data are reasonably consistent, e.g. values of $E_1^0 + 0.0197 \log k_d$ and E_1^0 in Table 1. It should be noted that the value of $E_1^0 = -1.13$ V (SCE) for the $NAD^+/NA\dot{D}$ redox couple derived from the polarographic measurements is in fairly good agreement with that of $E_1^0 = -0.922$ V (NHE), i.e. $E_1^0 = -1.16$ V (SCE), inferred from pulse radiolysis experiments [16].

The kinetic parameters of the electron-transfer step, k_1^0 and α_1, can be reliably evaluated from polarographic data only at higher NAD^+ concentration; $k_1^0 = 2 \times 10^{-2}$ cm s^{-1} was evaluated by eqn. (35), using $E_{1/2}^{irr} = -0.97$ V, $\alpha_1 = 0.5$ at

TABLE 1

Comparison of formal potentials for $NAD^+/NA\dot{D}$ couple based on polarographic and cyclic voltammetric measurements [a]

Method	$c^0_{NAD^+}$/mM	$(E^0 + 0.0197 \log k_d)$/V	E^0/V	Ref.
DME	0.013	−1.003	−1.130	9
	0.026	−1.003	−1.130	
	0.053	−0.994	−1.121	
	0.132	−0.982	−1.109	
CV	0.20	−0.996	−1.123	11
	0.40	−0.996	−1.123	

[a] The DME polarographic data from Fig. 3A [9] were used with the assumption that, at low NAD^+ concentration, $E_{1/2} = E_{1/2}^{rev}$. The diffusion layer thickness δ was calculated by eqn. (13); E_1^0 was calculated using $k_d = 2.7 \times 10^6$ M^{-1} s^{-1}.

$c^0 = 0.75$ mM (cf. Fig. 2) and $E_1^0 = -1.123$ V. A rough estimate of k_1^0 from fast-scan cyclic voltammetry ($I_{pa}/I_{pc} \simeq 1$ for $c^0 = 0.2$ mM) is 1×10^{-1} cm s^{-1}.

Parameters for mechanistic model for NAD·/NADH couple

For the NAD·/NADH couple, E_2^0, calculated from E^0 of -0.295 V for the NAD$^+$/NADH couple using eqn. (69), is 0.533 V.

The DME cathodic wave II, corresponding to reduction of NAD· to NADH, occurs at potentials as negative as -1.6 V; its log analysis (Fig. 4) yields a reciprocal slope of 108 mV. It is apparent that, if the reduction of NAD· proceeds according to eqn. (3), it must be quite irreversible, although the wave is also shifted negatively by the effect of the preceding dimerization reaction.

Equations (50) or (55) are relevant for analysis of wave II; the reciprocal slope of the $\log[I(I_1)^{-1/3}(I_1 - I)^{-2/3}]$ vs. E plot should be $2.303RT/\alpha_2 F$. The dependence of $E_{1/2}$ on NAD$^+$ concentration c^0 is expected to be characterized by eqn. (52), while the dependence of $E_{1/2}$ on pH is described by eqns. (53) or (57). In the latter case, i.e. for the mechanism involving the protonation of NAD· (eqns. 5 and 6), the inequality $k_H c^0_{H_3O^+}/c^0_{H_2O} \ll 1$ should hold, as previously discussed.

The indicated I–E plot (Fig. 4) is practically linear with a reciprocal slope of 120 mV, which corresponds to $\alpha_2 = 0.5$. Here, $E_{1/2}$ is linearly dependent on $\log c^0$ (Fig. 3B) with a slope of -37 mV, in excellent agreement with that of $-2.303RT/3\alpha_2 F = -39$ mV expected for $\alpha_2 = 0.5$.

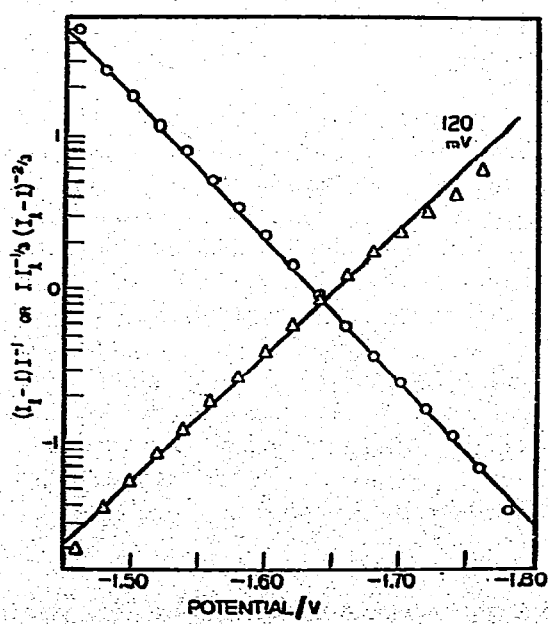

Fig. 4. (○) Plots of $\log[(I_1 - I)I^{-1}]$, and (△) of $\log[II_1^{-1/3}(I_1 - I)^{-2/3}]$ vs. potential E for the more negative cathodic wave of NAD$^+$ (0.745 mM).

Since the effect of pH on $E_{1/2}$ can only be investigated in the narrow range of pH 9–10 [9,10], a reliable slope cannot be inferred. The dependence of E_p can be measured more easily [10]; based on three points between pH 7.2 and 9.3, $\Delta E_p/\Delta$pH is −21 mV [10].

Obviously, both mechanisms suggested for the reduction of NAD· only qualitatively explain the effect of pH; both eqns. (53) and (57) predict a slope $\Delta E_{1/2}/\Delta\text{pH} = -2.303RT/\alpha_2 F = -120$ mV for $\alpha_2 = 0.5$. The problem is probably due to the simultaneous involvement of different proton donors such as the buffer components [10]. In fact, since the increase in H_3O^+ concentration is controlled by the decrease in concentration ratio of proton donor to proton acceptor of the buffer system, the changes may mutually compensate each other in the effect on the NAD· reduction rate. The involvement of other proton donors in the NAD· reduction is strongly supported by the effect of NH_4^+ ion concentration, i.e. $\Delta E_{1/2}/\Delta \log c^0_{HX} \simeq 100$ mV for $HX \equiv NH_4^+$ [10].

The subsequent calculation of k_2^0 is therefore limited by the assumption that H_3O^+ is the only proton donor. The value obtained, which can be revised when new results are available, is used in the following section to illustrate possible consequences resulting from the type of mechanism considered.

If the reduction of NAD· is assumed to proceed according to eqn. (3), k_2^0 can be calculated from eqn. (51). Using $E^{irr}_{1/2} = -1.634$ V at $c^9 = 0.745$ mM, $E_2^0 = 0.533$ V, $k_d = 2.7 \times 10^6\ M^{-1}\ s^{-1}$ and $\alpha_2 = 0.5$, a value for $k_2^0 c^0_{H_3O^+}$ of 1.5×10^{-20} cm s^{-1} is obtained at pH 9.1, from which $k_2^0 = 1.9 \times 10^{-11}$ cm s^{-1} M^{-1} (activity coefficient of $H_3O^+ = 1$).

EVALUATION OF PROPOSED MECHANISTIC MODEL

The preceding discussion indicates that the mechanism represented by eqns. (2)–(4) or that involving protonation of NAD· (eqns. 5 and 6) constitute a reasonable basis for qualitative interpretation of the electrochemical behavior of the NAD^+/NADH redox couple. The quantitative explanation is less satisfactory, particularly in respect of the effect of proton donor on reduction of NAD·. This does not necessarily mean that the mechanism should be revised, as the effect of a single proton donor has not so far been thoroughly investigated except for NH_4^+ [10]. Unfortunately, in the latter case, cross-data on the effect of NAD^+ concentration are not available. However, the effect of NH_4^+ itself indicates the experiments which should be undertaken in order to understand better the electrochemical behavior of the NAD^+/NADH couple, particularly as contrasted to its biological behavior.

Subsequent discussion considers some consequences of the proposed mechanism based on the quantitative parameters evaluated for the mechanistic model.

Reduction of NAD^+

The dependences of parameters a and b on the electrode potential E for several values of k_1^0 and k_2^0 for the mechanistic model represented by eqns. (2)–(4) were calculated (Fig. 5A), using eqns. (16)–(22).

The previous theoretical analysis indicated that the dimensionless current J generally satisfies inequalities (31) or (43) for the cathodic reaction and (63) or (65) for the anodic reaction. Based on the values of the kinetic parameters, the potential E^*, corresponding to the intersection of functions a and b, can be found and the functions $2p/(1+p)$ and $2q'/(1+q')$ plotted.

For $k_1^0 = 2\times10^{-2}$ cm s^{-1} and $k_2^0 = 1.9\times10^{-11}$ cm s^{-1} M^{-1}, $E^* = -1.24$ V. For the cathodic reaction, the current–potential curve in the potential region $E > -1.24$ V is given by eqn. (32). The function $2p/(1+p)$ for $k_1^0 = 2\times10^{-2}$ cm s^{-1} is shown in curve c_2 of Fig. 5B; it is apparent that E can be made sufficiently negative so that $p \gg 1$ in this region. Therefore, the current reaches the limiting value given by eqn. (33) and the current–potential curve is described by eqn. (34), which was actually used in the analysis of NAD$^+$ wave I (cf. dotted curve for Hg in Fig. 5B).

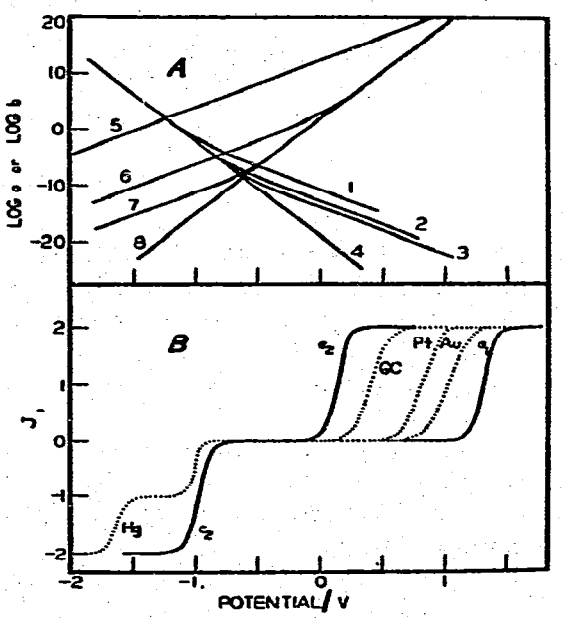

Fig. 5. (A) Variation of the parameters a (curves 1–4) and b (curves 5–8) with potential E for several values of the apparent rate constants k_1^0 (cm s^{-1}): (1) 2×10^{-2}; (2) 2; (3) 20; (4) ∞]; and k_2^0 (cm s^{-1} M^{-1}): (5) 1.9×10^{-11}; (6) 1.9×10^{-1}; (7) 1.9×10^{4}; (8) ∞. Values of the other parameters: $\delta = 3.07\times10^{-3}$ cm; $D = 3.5\times10^{-6}$ cm^2 s^{-1}; $c^0_{H_2O} = 55.5$ M; pH = 9.1; $E_1^0 = -1.123$ V; $E_2^0 = 0.533$ V; $\alpha_1 = \alpha_2 = 0.5$. (B) Variation of the dimensionless current J with potential E for NAD$^+$ reduction and NADH oxidation. (For clarity, J is considered as negative for reduction and positive for oxidation, although in the text J is always expressed as a positive quantity.) (·····) Experimental cathodic waves of NAD$^+$ (0.745 mM) at a DME and experimental anodic waves of NADH at RDE (30 rps) of GC (1 mM NADH), Au (1.1 mM) and Pt (1.1 mM); (————): dependences of $2q'/(1+q')$ on E calculated for $k_2^0 = 1.9\times10^{-11}$ cm s^{-1} M^{-1} (a_1) and 1.9×10^{-1} cm s^{-1} M^{-1} (a_2); other parameters are the same as for Fig. 5A, except that $\delta = 8.1\times10^{-4}$ cm (cf. eqn. 12) and $D = 3.3\times10^{-6}$ cm^2 s^{-1}. Curve c_2 is the dependence on E of $2p/(1+p)$, calculated for $k_1^0 = 2\times10^{-2}$ cm s^{-1}, with the other parameters being the same as for Fig. 5A.

In the potential region $E < -1.24$ V, the current–potential curve is generally given by eqn. (45). Since the inequality $p \gg 1$ is satisfied in this region and $E_2^0 > E_1^0$, eqn. (50) is applicable for the analysis of NAD^+ wave II.

Oxidation of NADH

For the anodic reaction, the function $2q'/(1+q')$ for $k_2^0 = 1.9 \times 10^{-11}$ cm s^{-1} M^{-1} was calculated for a RDE (30 rps) (curve a_1 of Fig. 5B). Obviously, the current is negligible at $E < -1.24$ V. At $E > -1.24$ V, eqn. (66) applies. Analysis of the right-hand side of eqn. (66) shows* that $(3/4\lambda^2)^{1/2}a^{-1} \gtrsim 100$ at $E > -0.85$ V, where eqn. (66) can be simplified to

$$J = 2q'/(1+q') \tag{80}$$

The limiting anodic current I_1 is given by

$$I_1 = 2FAD\,\delta^{-1}c_C^0 \tag{81}$$

Thus, the anodic wave of NADH, corresponding to the set of parameters for the mechanistic model, which were evaluated from the data on reduction of NAD^+ at Hg, is, in fact, curve a_1 of Fig. 5B. For this wave $E_{1/2}$ should be independent of proton donor concentration.

Electrocatalysis via mediator action

The oxidation of NADH was investigated at GC, Pt and Au electrodes [13]. The rate of oxidation markedly depends on the state of the electrode surface, and the electron transfer proceeds to at least some extent through mediator redox systems located close to the electrode surface such as redox couples formed by oxygen adsorbed at Au and Pt surfaces, and by organic functionalities resulting from oxidation of a carbon surface.

The dimensionless current–potential curves for the NADH oxidation are shown by dotted lines in Fig. 5B. The $E_{1/2}$ values (0.40 V at GC, 0.82 V at Pt, 1.02 V at Au) are more negative than that of 1.32 V for curve a_1. This shift can be interpreted in terms of electrocatalysis of the rate-determining step (rds),

$$NADH + H_2O \rightarrow N\dot{A}D + H_3O^+ + e \tag{82}$$

by a mediator redox system as discussed in ref. 13. In the electrocatalytic mechanism, the electroactive redox couple is that of the mediator, which requires the kinetic analysis to be carried out with respect to the formal potential of the mediator redox system. However, the coupling of the catalyzed rds with the follow-up dimerization and with the $NAD^+/N\dot{A}D$ electrode reaction, can be analyzed at least formally on the basis of the mechanistic model proposed.

The electrocatalytic effects should be reflected in the magnitude of the rate

* For $k_d = 2.7 \times 10^6$ M^{-1} s^{-1}, $c_C^0 = 1$ mM and $\lambda^2 = 5.4 \times 10^2$, the value of the parameter a is inferred from Fig. 5A.

constant k_2^0. We shall therefore investigate the hypothetical situation that k_2^0 is increased by several orders of magnitude. Using the relations derived for the two mechanisms suggested, we shall try to predict the shape and the position of the anodic and cathodic waves corresponding to such an increase in k_2^0, as well as the conditions under which the reversible electrochemical behavior of the NAD^+/NADH couple can be found, such as are encountered under biological conditions.

First, let us assume that k_2^0 for charge-transfer reaction (3) is 10 orders greater than that evaluated from the data on reduction of NAD^+, i.e., $k_2^0 = 1.9 \times 10^{-1}$ cm s^{-1} M^{-1}, with the other parameters unchanged. Inspection of Fig. 5A reveals that in this case $E^* = -0.77$ V. With respect to the cathodic reaction, the current must clearly be practically negligible at $E > -0.77$ V (cf. curve c_2 of Fig. 5B). For $E < -0.77$ V, the current–potential curve is described by eqn. (45). Since $\lambda^2 = 5.4 \times 10^3$ for the DME, $c_A^0 = 0.745$ mM and $b < 10^{-4}$ (cf. Fig. 5A), the right-hand side of eqn. (45) $\gtrsim 100$ and eqn. (45) simplifies to

$$J = 2p/(1+p) \tag{83}$$

with the limiting cathodic current given by eqn. (44). Thus, the expected cathodic wave of NAD^+ coincides with curve c_2 of Fig. 5B. Qualitatively, this corresponds to the situation that the second electron uptake, eqn. (3), outruns dimerization of the intermediate radical so that only a single $2e$ cathodic wave should be observed.

For the anodic reaction, the current–potential curve, again given by eqn. (80), is shown as curve a_2 in Fig. 5B, for which $E_{1/2}$ is about 0.4 V more negative than the E_2^0 of 0.533 V.

Further increase in k_2^0 has no effect on the cathodic wave of NAD^+, as the cathodic reaction is now controlled by the rate of the first-electron uptake, eqn. (2), and the wave coincides with c_2 of Fig. 5B.

On the other hand, with increasing k_2^0, the anodic wave of NADH shifts towards more negative potential. Because E^* simultaneously shifts towards more positive potential (cf. Fig. 5A), at sufficiently large k_2^0 ($\gtrsim 10^5$ cm s^{-1} M^{-1}) the inequality $q' \gg 1$ may be satisfied in the potential region $E < E^*$ and the single $2e$ anodic wave may start to split into two $1e$ waves. The latter case corresponds to the situation that, with increasing electrode potential, the rate of oxidation of NAD to NAD^+ decreases and starts to be outrun by the dimerization of NAD.

When $k_2^0 = 1.9 \times 10^{-11}$ cm s^{-1} M^{-1}, increase in k_1^0 above 2×10^{-2} cm s^{-1} has practically no effect on the cathodic wave of NAD^+ (dotted line in Fig. 5B), and no effect on the anodic wave of NADH. However, when k_2^0 is sufficiently large, e.g. 1.9×10^{-1} cm s^{-1} M^{-1}, so that the reduction of NAD^+ is controlled by the first electron uptake (eqn. 2) (cf. curve c_2 of Fig. 5B), increase in k_1^0 shifts the single $2e$ cathodic wave of NAD^+ to more positive potential.

The limiting situation arises when both k_1^0 and k_2^0 are sufficiently large* that E^* coincides with $E^{0\prime}$ for the NAD^+/NADH redox couple (eqn. 71) and $p \gg 1$ or

* By estimation, $k_1^0 \gtrsim 200$ cm s^{-1} and $k_2^0 \gtrsim 10^9$ cm s^{-1} M^{-1}.

$q' \gg 1$ in the potential region close to E^*. In this case, irrespective of the mechanism of proton transfer in the reduction of NAD· to NADH, the cathodic wave of NAD^+ is given by

$$\frac{(J-1)^3}{\left[(1+P)J-2\right]^2} = \frac{3}{4\lambda^2 b^3}(1-P) \tag{84}$$

where P is given by

$$P = \exp\left[2F(E-E^{0\prime})/RT\right] = b/a \tag{85}$$

Analogously, the anodic wave of NADH is given by

$$\frac{(1-J)^3}{\left[2-(P^{-1}+1)J\right]^2} = \frac{3}{4\lambda^2 a^3}(P^{-1}-1) \tag{86}$$

Owing to the third power of b or a in eqn. (84) or (86), the right-hand side of these equation $\gg 1$, except if P is very close to unity*. Thus, eqns. (87) and (88) practically hold for the cathodic and anodic reactions respectively, and are the equations for the reversible $2e$ cathodic and anodic waves:

$$J = 2/(1+P) \tag{87}$$

$$J = 2/(1+P^{-1}) \tag{88}$$

This situation was sought in the electrochemical behavior of the NAD^+/NADH couple, based on its reversible behavior under biological conditions, but has not been found. The main reason is most probably the slow rate of reaction of the NAD·/NADH couple which requires transfer of the proton from or to a third species. This reaction can be successfully catalyzed in the anodic direction by a mediator redox system located at the electrode surface, and in the cathodic direction hopefully by the presence of a suitable proton donor. Once the rate of this reaction is sufficiently rapid, the rate of reaction of the NAD^+/NAD· couple becomes the limiting factor responsible for an even smaller decline of the electrochemical behavior of the system from the reversible level.

Experimentally observed adsorption phenomena, which may be of importance, are not covered by the mechanism considered; the question of double-layer effects has also not been discussed. Nevertheless, the main features of the electrochemical behavior of the NAD^+/NADH redox couple can be understood in terms of the proposed mechanism. In connection with the hydride transfer hypothesis used to account for the NAD^+/NADH redox couple under biological conditions, further effort should obviously be directed towards the further explication of the role of the proton in the electrochemical transformation of NADH to NAD^+ and vice versa.

---

* For $\lambda^2 = 5.4 \times 10^3$ (DME; $c^0 = 0.745$ mM), $3/4\lambda^2 b^3$ or $3/4\lambda^2 a^3 \simeq 10^{21}$ at $E = E^{0\prime}$. The right-hand side of eqns. (84) or (86) $\gg 1$ for $(1-P)$ or $(P^{-1}-1) \gtrsim \pm 10^{-19}$.

ACKNOWLEDGEMENT

The authors thank the National Science Foundation which helped support the studies described.

REFERENCES

1 P.J. Elving, C.O. Schmakel and K.S.V. Santhanam, Crit. Rev. Anal. Chem., 6 (1976) 1.
2 J. Moiroux and P.J. Elving, J. Am. Chem. Soc., 102 (1980) 6533.
3 J. Jacq, Electrochim. Acta, 12 (1967) 1345.
4 R. Brdička, V. Hanus and J. Koutecký, Progress in Polarography, Vol. 1, Interscience, New York, 1962, Ch. VII, p. 145.
5 V.G. Levich, Physicochemical Hydrodynamics, Prentice-Hall, Englewood Cliffs, 1962.
6 R. Bonnaterre and G. Cauquis, J. Electroanal. Chem., 32 (1971) 199.
7 J. Jacq, Electrochim. Acta, 12 (1967) 1.
8 P.P. Schmidt, in Specialist Periodical Report, Electrochemistry, Vol. 6, The Chemical Society, London, 1978, p. 128.
9 C.O. Schmakel, Ph.D. Thesis, The University of Michigan, 1971.
10 M.A. Jensen, Ph.D. Thesis, The University of Michigan, 1977.
11 W.T. Bresnahan, Ph.D. Thesis, The University of Michigan, 1980.
12 W.M. Clark, Oxidation–Reduction Potentials of Organic Systems, Williams and Wilkins, Baltimore, 1960, p. 487.
13 Z. Samec and P.J. Elving, in preparation.
14 M.L. Olmstead, R.G. Hamilton and R.S. Nicholson, Anal. Chem., 41 (1969) 260.
15 W.T. Bresnahan and P.J. Elving, J. Am. Chem. Soc., 103 (1981) 2379.
16 R.F. Anderson, Biochim. Biophys. Acta, 590 (1980) 277.